RSC Advances

ROYAL SOCIETY OF CHEMISTRY

www.rsc.org/advances

Preparation, characterization and bioavailability of oral puerarin nanoparticles by emulsion solvent evaporation method

Yin Zhang, Yong Li, Xiuhua Zhao*, Yuangang Zu*, Weiguo Wang, Weiwei Wu, Chen Zhong, Zhao Li

(Key Laboratory of Forest Plant Ecology, Northeast Forestry University, Ministry of Education, Harbin 150040, Heilongjiang, China)

Abstract:

To improve the water solubility and dissolution rate, puerarin (PUE) was nanocrystallized by an emulsion solvent evaporation (ESE) method, followed by freeze-drying. The optimization conditions of preparation process were obtained by single-factor method. Under the optimum conditions, PUE nanoemulsion with mean particle size (MPS) of 185.2 ± 39.8 nm and polydispersity index value (PI) of 0.005 were prepared. PUE nanosuspension with an MPS of 67.9 nm (PI=0.280) was obtained after removing solvent by rotary evaporation. Puerarin nanoparticles (PUENs) with an MPS of 132.6 nm (PI=0.173) and zeta potential of 23.60 ± 2.55 mV were successfully prepared via further freeze-drying. PUENs were characterized by SEM, TEM, FTIR, XRD, DSC, TGA, equilibrium solubility, dissolution rate, oral bioavailability, hemorheology, cytotoxicity and solvent residue analysis. These results showed PUENs had a smaller particle size lower than raw PUE, and were changed into amorphous structure from crystal structure of raw PUE. The solubility and dissolution

* Corresponding author. Tel.: +86-451-82191517; fax: +86-451-82102082.
E-mail address: xiuhuazhao@nefu.edu.cn (Xiuhua Zhao).
* Corresponding author. Tel.: +86-451-82191517; fax: +86-451-82102082.
E-mail address: yuangangzu@163.com (Yuangang Zu)

rate of PUENs were significantly improved in simulated gastric fluid (SGF), simulated intestinal fluid (SIF) and deionized water compared with raw PUE. The oral bioavailability of PUENs was 2.83 times of raw PUE. PUENs improved hemorheology and did not enhance the cytotoxicity on normal cells. The residual amounts of ethyl acetate and ethanol were separately less than ICH limit for class III solvents. According to the results above, PUENs show the potential application value on its oral absorption.

Keywords: Puerarin; Emulsion solvent evaporation; Nanoparticles; Oral formulation; Solubility; Bioavailability

1. Introduction

Puerarin, a major isoflavonoid derived from the Chinese medical herb Radix Puerariae (kudzu root), has been documented to have numerous biological activities, such as antioxidant, hepatoprotective, estrogenic effects (1, 2) and anticancer activity (3). It is precisely because of such many beneficial physiological activities that it is widely prescribed for patients with diabetes mellitus (4) and cardio-cerebrovascular diseases (5), including myocardial ischemia (6), angina pectoris, arteriosclerosis (7), cerebral ischemia (8), and hypertension (9) in the world. However, PUE, as a Class IV drug in Biopharmaceutics Classification System (BCS) (10, 11), encounters poor water solubility and low oral bioavailability which strictly restrict clinical application. Pharmacokinetic studies indicated that the oral bioavailability of PUE was very low (<3%) (11). Now PUE is administrated mainly by vein injection in clinic. To solve the low water solubility issues, 1, 2-propanediol as a co-solvent was added into the current PUE injection formulation. Unfortunately, 1, 2-propanediol and its metabolites may be one of the sensitizing agents, leading to side effects, such as pruritus, chest tightness and shortness of breath (11). Hence, increasing the water solubility of PUE, enhancing the impact of its oral absorption, and improving its lower oral bioavailability are issues that need to be addressed urgently.

Researchers have been increasingly paying attention to new solubilization technologies, such as synthetic water-soluble prodrug, cyclodextrin inclusion (12), anionic polymerization (13), solid lipid nanoparticle (14), microemulsions (15), phospholipid complex (16) to improve the efficacy of poorly soluble drugs.

Nanoparticles preparation technique was first introduced into pharmaceutical field in the early time of 1990s, and quickly got researchers' attention from then on. So far, there are already several

commercial drug products based on drug nanoparticles technology, and more than twenty drug products are in different clinical stages (17-19). With the development of nanotechnology, this technique has become an important aspect in pharmaceutical research. In 2012, Wang used nanosuspension technique on PUE (20), but this work only focused on intravenous administration. Tu and Yi prepared PUE nanocrystals and microcrystals by using the high pressure homogenization method for oral administration in 2013 (11). But they only focused on pharmacokinetic studies of different particle size micro- and nano-crystals, not preparation process of nanocrystals.

In this study, to our knowledge, puerarin nanoparticles (PUENs) were first prepared using emulsion solvent evaporation (ESE) method, which has not been reported in literature up to now. Single-factor method of six main parameters affecting the mean particle size (MPS) was used to optimize the preparation of nanoparticles. The physico-chemical properties of PUENs powder obtained were characterized by scan electronic microscope (SEM), Transmission electron microscopy (TEM), Fourier transform infrared spectroscopy (FTIR), X-ray diffraction (XRD), differential scanning calorimetry (DSC), thermal gravimetric analysis (TGA), dissolution test and solvent residual determination. Cytotoxicity *in vitro*, oral bioavailability *in vivo* and hemorheology as essential assessments were also performed.

2. Material and methods

2.1. Materials

PUE (purity = 99.2%) was obtained from Shanxi Sciphar Hi-tech Industry Co., Ltd. (Shanxi, PR China). Poloxamer 188 was obtained from Hubei Hong Qi Chemical Co., Ltd. (Hubei, PR China). Ethanol, ethyl acetate and other organic reagents were obtained from Sigma-Aldrich Co. LLC. (St.

Louis, MO, USA). Methanol and acetonitrile were all HPLC-grade.

2.2. Preparation of PUENs

PUENs were prepared by ESE method, and followed by freeze-drying. A flow chart of the experimental processes to prepare PUENs was shown in Fig. 1. In the process, ethyl acetate containing 30% (v/v) ethanol as co-emulsifier was the organic phase of emulsions. The following detailed operation parameters were depended on single factor experiments. A certain amount of raw PUE powder was completely dissolved in the organic phase with concentration of 20 mg/mL. The obtained drug solution was slowly added dropwise to deionized water containing a certain concentration of poloxamer 188, a high macromolecule non-ionic surfactant with average molecular weight between 7,680 and 9,510, as surfactant under a vigorous stirring by using an FSH-II Adjustable High-Speed Homogenizer Stirrer (Jiangsu Zhengji Instruments Co., Ltd., Jintan City, PR China) at room temperature. Then, the obtained primary emulsions was homogenized in a high pressure nano homogenizer (AH-100D, ATS Engineering Inc., Vancouver, Canada), generating the nanoemulsions. The organic phase was removed by rotary evaporation using a rotary evaporator (R205, Shanghai Shensheng Biotech Co., Ltd., Shanghai, PR China) at an evaporation temperature of 40 °C. The remaining nanosuspension was freeze-dried at -50 °C for 48 h. The resulting was the desired PUENs.

2.3. Optimization of the ESE process

In this study, a single-factor method was used to determine the optimal conditions of PUE nanoemulsions by ESE process. Through the preliminary experiment, six main variables were picked out, included volume ratio of water to organic phase, the concentration of surfactants, speed and

duration of homogenate as well as homogenization pressure and cycles at certain pressures. The volume ratios of water to organic phase tested ranged from 2:1 to 5:1. The range of poloxamer 188 concentration tested was from 1 to 4 mg/mL (1‰ - 4‰). The homogenate speeds tested ranged from 4,500 to 10,500 rpm, and the duration of each time ranged from 1 to 7 min. The homogenization pressures were from 100 to 700 bar. And the homogenization cycles ranged from 2 to 14. All specific parameters and results are shown in Table 1. The optimum condition for every factor was determined based on the smallest MPS.

2.4. Characterization of PUENs

2.4.1. Morphology

The states of the emulsified system after homogenate and high-pressure homogenization were respectively observed by optical microscope (Olympus Corporation, BH-2, Tokyo, Japan). Before and after the freeze-drying, the morphology of the PUENs dispersed in deionized water were evaluated as well (3). Furthermore, the surface morphology of raw PUE and PUENs powder was ascertained by SEM (S4800, Hitachi, Ltd., Tokyo, Japan). The suitable amount of powders was fixed on the surface of the aluminum stub by using the carbon tape, respectively. Before analysis, the samples were sputter coated with gold under an argon atmosphere. TEM (H-7650, Hitachi, Ltd., Tokyo, Japan) was used to detect the morphology of PUENs. Samples were mounted on a microgrid carbon polymer supported on a copper grid by placing a few droplets of PUENs aqueous dispersions on the grid, followed by drying under ambient conditions, all in an Ar glovebox. The samples were transferred to the microscope in a special vacuum-transfer sample holder under exclusion of air.

2.4.2. *Mean particle size* and zeta potential *analysis*

The MPS and zeta potential of the obtained emulsions and nanoparticles were analyzed by dynamic light scattering (DLS) equipment (ZetaPALS, Brookhaven Instruments, Long Island, NY, USA). The samples of PUE primary or nano-emulsions obtained were analyzed directly. The samples of PUENs powder were prepared by dispersing in deionized water under an ultrasonic bath. Each experimental preparation was executed in triplicate, and data were obtained from the average of three measurements.

2.4.3. *Fourier transform infrared spectroscopy (FTIR)*

The surface chemical character of poloxamer 188, raw PUE, PUENs, physical mixture of raw PUE and poloxamer 188 at the same mass ratio as PUENs (MIX-PUE) were detected through FTIR by use of IRAffinity-1 spectroscope (Shimadzu Corporation, Tokyo, Japan). The samples were diluted with KBr mixing powder at 1% and pressed to self-supporting discs respectively. The FTIR spectra were obtained in KBr discs. The analytical range of the spectra at room temperature was from 4000 to 400 cm^{-1} at the resolution of 2 cm^{-1}.

2.4.4. *X-ray diffraction studies (XRD)*

The XRD patterns were used to confirm the crystal forms of poloxamer 188, raw PUE, PUENs and MIX-PUE, which were recorded by use of a Cu target tube at 30 mA and 40 kV with an X-ray diffractometer (Philips, X'pert-Pro, Amsterdam, The Netherlands) with a rotating anode. The scanning rate (5 °/min) was constant for all XRD analysis. The scanning ranged from 5 ° to 60 ° with a step size of 0.02 °.

2.4.5. Differential scanning calorimetry (DSC)

DSC (TA instruments, DSC 204, Woodland, CA, USA) was conducted for poloxamer 188, raw PUE, PUENs and MIX-PUE. Five milligrams of the sample was weighed into the sample pool to be scanned from 45 to 300 °C at a rate of 10 °C/min under N_2 atmosphere.

2.4.6. Thermal gravimetric analysis (TGA)

TGA of poloxamer 188, raw PUE, PUENs and MIX-PUE were performed by a Thermo-gravimetrical Analyzer (Diamond TG/DTA from Perkin–Elmer, Waltham, MA, USA) at a heating rate of 10 °C/min using a nitrogen purge. The heating temperature of samples weighing 3-5 mg ranged from 50 to 500 °C.

2.4.7. Residual solvent determination

The residual ethyl acetate and ethanol in the PUENs were analyzed using an Agilent 7890A gas chromatograph (Agilent Technologies, Palo Alto, CA, USA) with DB-WAX polyethylene glycol capillary column (30.0 m×250 μm×0.25 μm, nominal) equipped with a G1540N-210 FID detector. PUENs (50 mg) were dissolved in 0.6 mL of chloroform in an ultrasonic bath for 30 min, followed by centrifuging at 10000 g for 5 min. Peaks areas were used for obtaining quantitative data. The conditions of GC analysis of chromatograph were as follows: oven temperature was maintained at 40 °C for 5 min initially, and then raised at the rate of 10 °C/min to 200 °C, which was maintained for 3 min at last. The injector and the detector temperatures were set 200 °C and 250 °C, respectively. Nitrogen was used as carrier gas at a flow rate of 25 mL/min, and 2 μL samples were injected manually in the split mode with a split ratio 25:1. Hydrogen gas and air flow rate were 30 and 400

mL/min.

2.4.8. Equilibrium solubility study

In this test, raw PUE and PUENs were compared qualitatively by the USP apparatus (II) paddle method. Simulated gastric fluid (SGF) without enzymes was made by mixture of 5 mL 37% hydrochloric acid and 1000 mL deionized water (21), simulated intestinal fluid (SIF) without enzymes was composed of 6.8 g/L KH_2PO_4 (22, 23), adjusted to pH 6.8 with NaOH and deionized water, which were used as the dissolution medium. The paddle speed and bath temperature were set at 100 rpm and 37.0 ± 0.5 °C, respectively. Raw PUE (100 mg), PUENs (containing 100 mg PUE) and MIX-PUE (containing 100 mg PUE) were added to 5 mL of each dissolution medium for 48 h, respectively. In the pre-experiments, the nanoparticles completely dissolved in all dissolution mediums after 24 h. In the formal experiments, we made it 48 h for sure. After 48 h, samples (1 mL) were withdrawn and centrifuged at 12,000 g for 10 min. Then 10 μL of the supernatant was directly injected into the HPLC system and assayed for PUE concentration. The analysis condition is as follows: The drug concentration was determined by a Waters HPLC (Waters Corporation, Milford, MA, USA) consisting of a pump (Waters 1525 binary) and UV detector (Waters 2478 Tunable Absorbance Detector), which was equipped with the DIKMA Diamonsil C_{18} column (5 μm, 4.6 mm × 150 mm). The integrator system is Breeze 2. The mobile phase, consisted of 30% acetonitrile, 70% deionized water, was delivered at 0.8 mL/min. The samples were detected at 250 nm. The experiment was conducted in triplicate.

2.4.9. Dissolution rate study

The dissolution study of raw PUE, PUENs and MIX-PUE was performed by dialysis method.

The paddle speed was set at 100 rpm at bath temperature of 37.0 ± 0.5 °C. SGF and SIF without enzymes were used as the dissolution medium. Raw PUE (195.1 mg in SGF; 438.8 mg in SIF), PUENs and MIX-PUE (both containing the same mass of PUE) were respectively loaded in two same dialysis bags with 5 mL dissolution medium, which were immersed in 250 mL dissolution medium. Samples (5 mL) in dissolution medium were withdrawn at 5, 15, 30, 60, 120, 240, 360, 480, 600, 720 and 1,440 min, and filtered by 0.22 μm filters. After each sampling the same volume of dissolution medium was supplemented immediately. The filtrate samples were directly injected into the HPLC system and then the PUE concentration was assayed. The analysis conditions were the same as described in last section. The experiment was repeated three times.

2.4.10. Stability study of PUENs

The stability study of PUENs was detected to analysis crystalline state by performing XRD. The sample was stored in a dryer at room temperature for 12 months. Three samples were sampled at 0 day, 180 days, and 365 days to analyze, respectively. The analysis conditions were the same as described in Section 2.4.4.

2.5. In vitro cytotoxicity test

2.5.1. Cell culture

The IEC-6 cells (ATCC® CRL-1592™, rat intestinal crypt epithelial cell line) were obtained from the American Type Culture Collection (Manassas, VA, USA). PUENs as an oral dosage form are mostly absorbed in the small intestine; therefore, the IEC-6 cells were chosen as an *in vitro* model system to study the cytotoxicity of PUENs. The cells were cultured in DMEM containing 4

mM L-glutamine and 4.5 g/L glucose and supplemented with 10% fetal bovine serum (CLARK Bioscience LLC., Houston, TX, USA) in a humidified incubator at 37 °C under a 5% CO_2 atmosphere, and the medium was replaced with fresh medium every 2 days.

2.5.2. MTT assay

In vitro cytotoxicity test was performed by using MTT assay to assess the cell viability of IEC-6 cells. The exponential growth-phase IEC-6 cells were seeded into 96-well plates at 1×10^4 cells/well (200 μL) and cultured in a 5% CO_2 incubator at 37 °C for 24 hours. The samples containing PUENs and raw PUE were added into wells at different concentrations (0.1, 1, 10, and 100 μg/mL), respectively. Each concentration was repeated six times. After the incubation for 48 h, 10 μL of MTT solution (5 mg/mL) was added to each well and the reaction mixture was incubated for another 4 h. The supernatant was discarded and 150 μL DMSO was added into each well. The 96-well plates were put on a horizontal oscillator to increase the solvation of formazan crystals. The optical density (OD) values were determined by a microplate reader (SpectraMax i3x, Molecular Devices, LLC., Sunnyvale, CA, USA) at the wavelength of 570 nm. The cell viability was expressed as the percent of the control group.

2.6. Oral bioavailability study

2.6.1. Animals and treatment

Sprague–Dawley female rats were provided by Harbin Medical University (Harbin, Heilongjiang, PR China). 12 female Sprague-Dawley rats, weighing 200-250 g were used in this study. Rats were randomly divided into two groups, each with six animals. Animals were housed

under standard conditions of temperature, humidity, and light with food and water provided freely and allowed to acclimatize in the laboratory for at least 1 week prior to the experiment. Before administration, the animals were fasted overnight with free access of water. The animal use and care protocol was reviewed and approved by the ethics committee of the Harbin Medical University, including the subsequent experiments on rats.

Raw PUE was dispersed into 1% (w/v) HPMC-water solution and PUENs was dispersed in deionized water evenly. For the oral bioavailability study, two groups of male rats (n=6) were administered with an oral dose (100 mg/kg PUE by gavage). Blood samples by puncture of the orbital venous sinus were collected into heparinized tubes before and at 5, 15, 30, 60, 120, 240, 360, 480, 600, 720 and 1,440 min after oral administration according to Tu's research (11). The samples were immediately centrifuged at 3,000 g for 10 min and aliquots of plasma were stored at -20 °C until additional extraction and analysis.

2.6.2. Preparation of plasma sample

The treatment of frozen samples after being thawed at room temperature were referred to Tu's research (11) and as follows: each 200 μL plasma sample was combined with 400 μL methanol and vortexed for 3 min. Followed by ultrasonic treatment for 10 min and being centrifuged at 12,000 g for 10 min, 10 μL of the supernatant was injected for HPLC analysis. The analysis conditions were the same as described in Section 2.4.8. The oral bioavailabilities of samples are represented by the area under the plasma concentration–time curve (*AUC*).

2.7. Hemorheology study

Thirty male Sprague–Dawley rats with weight of 200 ± 20 g were divided into 3 groups

247 randomly, control group, raw PUE group and PUENs group (n=10). All the groups were
248 administrated by oral dose for 30 days (100 mg/kg PUE, once a day) except the control group was
249 administrated with deionized water at the same volume of experimental groups. All rats had common
250 feedstuff and drank water freely, and weighted once a week. One hour after the final dose, 5 mL
251 blood of each rat was taken from heart by using a heparin anticoagulant vacuum blood collection
252 tube. The whole blood viscosity and whole blood reduced viscosity under high, middle and low
253 shear force, plasma viscosity, hematocrit, erythrocyte aggregation index, erythrocyte rigidity index,
254 erythrocyte deformation index and erythrocyte electrophoresis index were detected by automatic
255 hemorheology meter (LBY-N6K, Beijing Precil Instrument Co., Ltd., Beijing, PR China).

256 **3. Results and discussion**

257 ***3.1. Optimization study***

258 Particle size of water-insoluble drug powder plays a key role in the improvement of solubility
259 (24). So particle size was chosen as response value in the optimization process. During preliminary
260 experiments, we determined that the following factors had a significant effect on the MPS of PUE
261 emulsions: volume ratio of water to organic phase; the concentration of surfactants; homogenate
262 speed and time as well as homogenization pressure and cycles. The effects of above factors on the
263 MPS were determined using a single-factor array (as seen in Table. 1).

264 ***3.1.1. Ratio of water* to organic phase**

265 The first factor was volume ratio of water to organic phase. The ratios were examined to be
266 within the range of 2:1 to 5:1. From Fig. 2 (a), it can be clearly seen that with the increasing volume

ratio of water to organic phase, the MPS of PUE emulsions fluctuated between 207.5 ± 76.8 and 469.0 ± 34.4 nm. This is caused by the influence of phase volume ratio on the emulsions droplet size. Finally, 2.5:1 was selected as the optimal proportion of water to organic phase to form a stable emulsions system and be used in subsequent tests.

3.1.2. Surfactants concentration

Based on the assessment of emulsification effect and freeze-dried state in preliminary experiment, poloxamer 188 (25) was selected among several surfactants. Poloxamer 188 is generally regarded as nontoxic and nonirritant materials, and it is not metabolized in the body. According to the available data about acute animal toxicity, its LD_{50} (rat, oral) is 9.4 g/kg. The concentration of poloxamer 188 (26) in water phase was the second factor to be considered. Fig. 2 (b) showed the effects of the concentration of surfactant on MPS. When the amount of poloxamer 188 increased from 1 to 4 mg/mL, the MPS of PUE emulsions decreased firstly and increased subsequently. The MPS of PUE emulsions decreased obviously from 363.6 ± 77.6 to 236.9 ± 11.9 nm as the concentration of poloxamer188 ranged from 1 to 1.5 mg/mL, then increased to about 400 nm with increasing concentration of poloxamer 188. A certain concentration of surfactant in the water phase is beneficial to reduce the interfacial tension, stabilizing formed emulsions and hindering particles aggregation, as a result of decreasing of particle size. However, when the concentration of surfactant was increased to a certain degree, the viscosity of water phase increased, making particles difficult to disperse, accompanied by the increase of particle size. Therefore, the optimum concentration of poloxamer 188 was selected to be 1.5 mg/mL.

3.1.3. Homogenate speeds and time

From the Fig. 2 (c), the MPS of PUE emulsions decreased from 280.4 ± 53.9 to 174.7 ± 49.9 nm with the increasing of homogenate speeds from 4,500 rpm to 6,500 rpm, followed by a significant increase of MPS when the homogenate speeds up to 7,500 rpm until 10,500 rpm. When the homogenate speed was under 6,500 rpm, the intensity of mass transfer between two phases was too small to adequately mix up water phase and oil phase, without realizing emulsifying effect. Nevertheless, excessive homogenate speed damaged the stability of emulsions to bring about the increase of particle size. Therefore, the optimum homogenate speed was selected to be 6,500 rpm.

The effect of homogenate time was shown in the Fig. 2 (d). The MPS of PUE emulsions decreased significantly from 552.9 ± 100.9 to 389.3 ± 42.0 nm with the increasing of homogenate time from 1 to 3 min, followed by a steady increase of MPS to 622.4 ± 92.1 nm with the homogenate time prolonging to 7 min. It was determined that it was not useful to homogenize at 6,500 rpm for a long period. Further, a longer homogenizing time may break the stability of the droplets, resulting in a larger particle size (27). Therefore, the optimum homogenate time was determined to be 3 min.

3.1.4. Homogenization pressure and cycles

Homogenization can ensure a smaller particle size (28) and a more uniform droplet (29). A sample was prepared under the optimal conditions just described to study the impact of homogenization pressure and cycles on MPS. First, we tested homogenization pressures in the range of 100-700 bar as it was shown in Fig. 2 (e). The MPS of PUE emulsions decreased from 289.5 ± 24.0 to 148.4 ± 27.1 nm when the homogenization pressure increased from 100 to 500 bar with a small fluctuation at 400 bar. Then the MPS became larger when the homogenization pressure

increased over 500 bar. The increase of homogenization pressure contributed to prevent the agglomeration of emulsions droplets to form small particle size. However, homogenization pressure was increased to a certain degree and demulsification would follow. Thus, 500 bar was selected as the optimal homogenization pressure.

Homogenization cycles as the final optimize parameter were tested between 2 and 14 as it was shown in Fig. 2 (f). At first the MPS of PUE emulsions decreased from 458.7 ± 85.9 to 185.2 ± 39.8 nm with homogenization cycles were increased from 2 to 8, although there was a fluctuation at 4 cycles. When homogenization cycles exceeded 8, the MPS of PUE emulsions increased. The increase of homogenization cycles prolonged the emulsification time at high pressure, which benefited the formation of small and uniform nanoemulsions droplets. Meanwhile, small and uniform nanoemulsions droplets had large surface area. The limited poloxamer 188 could not be effectively adsorbed to the particle surfaces, thereby reducing the emulsification, aggregating the droplets, increasing the particle size and causing instability. Ultimately, we chose 8 cycles as the optimal number of homogenization cycles.

Data were statistically evaluated by using variation coefficient method. By comparing the coefficient of variation (CV) (as shown in Table. 1), the grades of influence by six parameters were as followed (from big to small): homogenization cycles (50.4%), homogenate time (42.6%), homogenate speeds (32.1%), homogenization pressure (29.2%), ratios of water to oil phase (27.5%) and concentration of poloxamer 188 (18.4%).

3.1.5. Validation of the optimal conditions

According to the results of single-factor experiments above, the optimal conditions were as

followed: 2.5:1 of volume ratio of water to organic phase, 1.5 mg/mL of poloxamer 188, 6,500 rpm of homogenate speed for 3 min and a homogenization pressure of 500 bar for 8 cycles. PUE nanoemulsions with MPS of 185.2 ± 39.8 nm (PI=0.005) were prepared under these conditions. PUE nanosuspension with an MPS of 67.9 nm (PI=0.280) was obtained after the solvent was removed by rotary evaporation. The reason why the MPS decreased should be that the drug was reconstructed to form nanoparticles with smaller particle size and no agglomeration during the removal process of oil phase using rotary evaporation. Followed by freeze-drying, PUENs with an MPS of 132.6 nm (PI=0.173) and zeta potential of 23.60 ± 2.55 mV were successfully prepared. The subsequent characteristics of the optimum sample were all obtained under these conditions.

3.2. Characterization of PUENs

3.2.1. Morphology, particle size and zeta potential

The morphology of the samples was shown in Fig. 3 and Fig. 4. The raw PUE appeared as irregular blocks, with particle size ranging from 1 to 200 μm in Fig. 3 (a). Fig. 3 (b) showed that PUENs presented a uniform nearly ellipsoid shape and were connected together, which was due to the polymer structure of poloxamer 188. PUENs had smaller particle size ranging from 50 to 100 nm. The normal distribution curves of fresh nanosuspension and freeze-dried PUENs under optimum condition were shown in Fig. 3 (c_1, d_1). Before and after the freeze-drying, spherical particles with a similar particle size distribution were observed by the light microscopy in Fig. 3 (c_2, d_2). The MPS of fresh nanosuspension and freeze-dried PUENs were 67.9 nm and 132.6 nm, respectively. The increasing of MPS could be attributed to the agglomeration of particles during freeze-drying process. As seen in Fig. 4, the TEM image shows PUENs were found nearly ellipsoidal in shape with an MPS

about 100 nm. This evidence was consistent with the result of the SEM image shown in Fig. 3 (b). In contrast, the MPS of PUE nanocrytals prepared using high pressure homogenization method by Liangxing Tu was 525.8 nm (11). In Tu's study, they just used PUE suspension with HPMC as a suspending agent to prepare PUE nanocrystals. Moreover, the preparation processes of PUE nanocrystals were not optimized. They paid close attention to pharmacokinetic studies of different particle size micro- and nano-crystals rather than the preparation process of nanocrystals. The zeta potential of PUENs was 23.60 ± 2.55 mV. It was generally believed that absolute zeta potential value of 20 mV was sufficient to maintain stable nanosuspension (30).

3.2.2. Surface chemical character

The molecular structures of raw PUE and PUENs were examined in the range of 400-4000 cm^{-1} with the FTIR. As seen from Fig. 5 (a) and Fig. 5 (c), raw PUE and MIX-PUE showed the same FTIR spectrum. However, some differences have been found in spectra curves of the raw PUE (Fig. 5a) and the PUENs (Fig. 5b). PUENs presented two remarkable absorption peaks at 3367 cm^{-1} and 2886 cm^{-1} due to poloxamer 188. This indicated poloxamer 188 as a surfactant could prevent the agglomeration of PUENs.

3.2.3. Physical structure characterization

X-ray diffraction was performed to further investigate the crystalline structure of particles. The corresponding results for poloxamer 188, raw PUE, PUENs and MIX-PUE were shown in Fig. 6A. As seen from Fig. 6A (b, d), PUE and poloxamer 188 were highly crystallized and showed intense crystalline peaks. Fig. 6A (c) showed the MIX-PUE had both crystalline peaks of PUE and poloxamer 188 with intensity changes. However, the PUENs did not present obvious peak in Fig. 6A

(a), which indicated that the vast majority of PUENs was present in the desired amorphous state accompanied by little crystal form.

The DSC analysis was used to further confirm the result of XRD. The results were shown in Fig. 7. The peak at 54 °C is the melting point of poloxamer 188 crystals as it was shown in Fig. 7 (d). In Fig. 7 (b), the curve of raw PUE showed three endothermic peaks, a peak at 106 °C and two peaks at 213 °C. The first peak could be attributed to its water loss and the other peak was closer to the melting point of PUE crystal. There was no difference between Fig. 7 (b) and Fig. 7 (c). In Fig. 7 (a), the peak at 247 °C is in accord with the melting point of a different crystal form of PUE (31). It is speculated that there was a different crystal form of PUE transformed in the heating process of DSC, since PUE has the property of polymorphism. Polymorphism is very common in drugs and different crystals of the same drug compound can lead to marked differences in appearance, solubility, melting point, density, dissolution, etc., which accordingly will affect its stability and bioavailability (31). There also is another possibility that a change of mesoform existed in this heating process. Furthermore, poloxamer 188 showed an endothermic peak at about 54 °C, while the peak disappeared in the thermogram of PUENs, which might be due to drug interfering in the heat flow. This evidence confirmed that PUENs was mainly present in amorphous structure, which was in accordance with the XRD results. In many studies, it has been reported that low crystalline form could enhance dissolution and bioavailability (32).

The TGA curves of raw PUE and PUENs were shown in Fig. 8. The raw PUE showed obvious thermal weight losses since 207 °C in Fig. 8 (b). However, the PUENs began to lose weight since 230 °C in Fig.8 (a), which was in accordance with the DSC results. Before 300 °C there was no significant difference of descent rate between raw PUE and PUENs, but after 300 °C PUENs lost

much more weight than raw PUE. This may be due to the fact that the smaller PUENs have a higher specific surface than raw PUE, which leads to easier vaporization and a faster thermal decomposition rate. Generally speaking, the overall trend of PUENs is almost consistent with the raw PUE.

3.2.4. Solvent residue analysis

The problem of solvent residues is also under consideration in pharmaceutical products. Fig. 9 showed the results of ethyl acetate and ethanol residue using the GC method. From the chromatograms of ethyl acetate and ethanol standard solutions, a regression equations between peak area (y_1) and ethyl acetate concentration (x_1) can be fitted as y_1=30205.5217x_1-30.3243, (R^2=0.9999); a regression equations between peak area (y_2) and ethanol concentration (x_2) can be fitted as y_2=34001.4502x_2+16.4365, (R^2=0.9992). The linear range of solvents was 0.003125-0.2 mg/mL. According to the regression equation, the residual ethyl acetate and ethanol content in PUENs were 9.3 ppm and 8.0 ppm, respectively. Since the International Conference on Harmonization (ICH) limit for ethyl acetate and ethanol in class III solvents is 5000 ppm or 0.5%, the PUENs met ICH requirements and are suitable for pharmaceutical use.

3.2.5. Equilibrium solubility

The equilibrium solubility of raw PUE, PUENs and MIX-PUE was shown in Fig. 10. The terminal solubility of raw PUE, PUENs and MIX-PUE were 2.18 ± 0.21, 3.90 ± 0.37 and 3.75 ± 0.27 mg/mL in SGF; 3.90 ± 0.28, 8.78 ± 0.61 and 6.38 ± 0.26 mg/mL in SIF; 1.72 ± 0.19, 7.05 ± 0.48 and 4.95 ± 0.20 mg/mL in deionized water, respectively. The equilibrium solubility of PUENs was increased 1.79 times in SGF, 2.25 times in SIF and 4.10 times in deionized water of raw PUE. The

equilibrium solubility of MIX-PUE in such three medium showed advantages compared with raw PUE. Meanwhile, PUENs were superior to MIX-PUE in equilibrium solubility. The results indicated poloxamer 188 enhanced the solubility of MIX-PUE to some extent, and high solubility of PUENs was primarily ascribed to the reduction of particle size and amorphous structure of PUE. Moreover, the nanoscale of PUE in PUENs played a more important role in improving the solubility.

3.2.6. Dissolution rate

The dissolution profiles of raw PUE, PUENs and MIX-PUE in two different dissolution medium were shown in Fig. 11 and Fig. 12. In SGF the three samples all presented the fastest release rate at different levels in the time interval of the initial 6 h, followed by gradual and sustained release until 24 h, as shown in Fig. 11. The dissolution percentages of raw PUE, MIX-PUE and PUENs almost achieved 55.29 ± 4.65%, 57.79 ± 3.75% and 92.94 ± 5.95% at 12 h., respectively. As for Fig. 12, all three samples exhibited similar dissolution characteristics up to 2 h in SIF. The dissolution rate of PUENs was obviously faster than raw PUE and MIX-PUE until 12 h. Moreover, the dissolution percentage of PUENs at 12 h almost achieved up to 100% which was nearly twice of raw PUE and. In conclusion, the dissolution rate of PUENs was the fastest, followed by MIX-PUE and raw PUE. The dissolution characteristic of PUENs was in accordance with the Higuchi equation of y=-12.2022$e^{(-x/0.1884)}$-89.5908$e^{(-x/5.4301)}$+101.2122, (R^2=0.9941) in SGF and y=101.61335/(1+58.0271$e^{(-0.64029x)}$), (R^2=0.9875) in SIF. The results showed that the drug dissolution of PUENs was in conformity with the first-order kinetics equation.

The introduction of poloxamer 188 acting as co-emulsifier in MIX-PUE accelerated the dissolution of PUE in some degree. According to Noyes-Whitney equation, the drug dissolution rate

435 is linear relationship to the surface area exposed to the dissolution medium (33, 34). Dissolution rate
436 of MIX-PUE and raw PUE did not differ much, since there was no change in particles size of
437 MIX-PUE, resulting in no change in surface area. The accelerated dissolution rate of PUENs could
438 be mainly attributed to their greater surface area induced by the great reduction of particles size (35).
439 Another reason for the increase of dissolution rate is the amorphous state of PUENs. The amorphous
440 state would lead to a higher surface disorder, resulting in higher equilibrium solubility as well as
441 dissolution rate than crystalline materials (36). Therefore, PUENs with amorphous structure have a
442 higher dissolution rate and solubility than raw PUE. In addition, PUENs powder can be made into
443 oral tablets which would improve oral bioavailability of PUE.

444 ***3.2.7. Stability study of PUENs***

445 The crystalline states of 0 day, 180 days and 365 days PUENs were shown in Fig. 6B. The
446 long-term data showed the PUENs in amorphous state had little change over time, which declared
447 that PUENs remained well for up to 365 days.

448 ***3.3. In vitro cytotoxicity test***

449 MTT assay was adopted to perform cytotoxicity test of IEC-6 cells with raw PUE and PUENs.
450 As shown in Fig. 13, all the cell viability of experiment groups were over 90%, which indicate that
451 the cell viability was not remarkable affected by raw PUE and PUENs under these concentrations.
452 The result shows PUENs did not change the biocompatibility of raw PUE on normal cells. In
453 addition, there was no significant difference among the tested concentration (p>0.05).

3.4. Oral bioavailability studies of PUENs in rats

The main pharmacokinetic parameters (C_{max}, T_{max}, $AUC_{(0-t)}$, $AUC_{(0-\infty)}$) were listed in Table 2 and the blood concentration–time curves of PUE suspension and PUENs suspension after oral administration in rats were shown in Fig. 14. The results showed the C_{max} was increased with the reducing of particle size, which could be explained as that comparing to raw PUE, the PUENs had a higher equilibrium solubility and dissolution velocity in digestive juice owing to their reduced MPS (28, 37). Hence, a high drug concentration gradient between gastrointestinal tract and blood vessel occurred, accompanied by distinctly enhanced absorption and a high C_{max}. The raw PUE and the PUENs groups attained their maximum of PUE concentration in rat plasma, namely 0.81 ± 0.09 and 3.63 ± 0.21 μg/mL after 1 h and 15 min of taking drugs, respectively. Moreover, there was a second peak value of 1.06 ± 0.10 μg/mL in PUENs group at 6 h. The bimodal phenomena of PUENs group may attribute to the different PUE forms in PUENs, which lead to the different absorption time. Fig. 15 shows the schematic diagram of *in vivo* drug release mechanism. *In vivo*, the vast majority amorphous PUEs first release and be absorbed into the system, then little PUE crystals release later. The oral relative bioavailability of PUENs was calculated by the ratio of the *AUC* values between PUENs and PUE groups, namely 12.20 and 4.31 mg/L·h. The *AUC* values indicated the oral bioavailability of the PUENs increased 2.83 times compared with the raw PUE. The significant enhancement of oral bioavailability is also in accordance with the results of the dissolution test and above characterization tests.

3.5. Hemorheology study

The objective of this study is to investigate the change of hemorheology in rats after oral

administration of raw PUE and PUENs. And all the measured parameters and data are shown in Table 3. The data shows that after 30 days of treatment PUENs improved whole blood viscosity and whole blood reduced viscosity obviously, and had better effect than raw PUE. And PUENs reduced erythrocyte aggregation and rigidity to some extent, which can improve microcirculation to restore blood supply. In conclusion, its contribution of improving hemorheology can effectively prevent the occurrence and development of cardiovascular disease. There is statistically significant difference of whole blood viscosity and whole blood reduced viscosity (high, medium, low shear rate) between PUENs group and control group (p<0.05).

There have been several methods to prepare nano-PUE in existing literatures. Luo (14) prepared PUE solid lipid nanoparticles by using the solvent injection method. Their MPS (160 nm) and the bioavailability increment (about 3 times) are similar to ours. However, the preparation of solid lipid nanoparticles needs high cost and phospholipids tends to be easily oxidized. According to Tu's research (11), PUE microcrystals (1875.6 nm) and nanocrystals (525.8 nm) were prepared by using high pressure homogenization method, with $AUC_{0\text{-}t}$ of 4.98 and 15.12 mg·h/L, respectively. The possible cause of difference on the oral bioavailability between Tu's and our research may be the experimental animals, HPMC as a kind of nanocrystals stabilizer and test error. Moreover, the drug content is only 50% and has low zeta potential. The long-term stability of this drug is not reported in this literature. By contrast, 84.21% of higher drug content, 23.6 mV of higher potential and good long-term stability emerged on the PUENs in this research. Furthermore, this research results indicate PUENs did not change the biocompatibility of raw PUE on normal cells and improved the hemorheology indexes of rats. In summary, this paper has conducted a more comprehensive and in-depth research on PUENs prepared by ESE method.

4. Conclusion

This study attempts to improve the oral bioavailability of PUE. PUENs were successfully prepared by emulsions solvent evaporation method, followed by freeze-drying. In this process, poloxamer 188 was used as surfactant and co-emulsifier. Single-factor experiment was used to obtain the optimal conditions for nanoparticles. The optimal conditions are as follows: 2.5:1 of volume ratio of water to organic phase; 1.5 mg/mL of poloxamer 188, 6,500 rpm of homogenate speed for 3 min and at a homogenization pressure of 500 bar for 8 cycles. PUENs were nearly ellipsoid with uniform particle size distribution. Solubility and dissolution test showed the enhanced dissolubility of PUENs. *In vivo* bioavailability study of drugs showed that PUENs had better absorption in the body, in which the relative oral bioavailability was increased 2.83 times compared with raw PUE. Results indicated that the nanoparticle drug system could improve the water solubility of PUE, promote the absorption of PUE *in vivo*, correspondingly along with the enhancement of oral bioavailability. PUENs improved hemorheology and did not enhance the cytotoxicity on normal cells compared to the raw PUE. In addition, the residual ethyl acetate is less than the ICH limits for class III solvents. In summary, this article provides a theoretical and experimental basis for solving poor water solubility and low oral bioavailability of PUE.

Acknowledgements

The authors are grateful for the precious comments and careful corrections made by anonymous reviewers. The authors would also like to acknowledge the financial support from the Fundamental Research Funds for the Central Universities (2572016AA49), the National Key Technology R&D Program (2012BAD21B0501), and the National Natural Science Foundation of China (No. 21473023).

519 **References**

520 1. Zhang S, Ji G, Liu J. Reversal of chemical-induced liver fibrosis in Wistar rats by puerarin. The
521 Journal of Nutritional Biochemistry. 2006;17(7):485-91.
522 2. Xia D-Z, Zhang P-H, Fu Y, Yu W-F, Ju M-T. Hepatoprotective activity of puerarin against carbon
523 tetrachloride-induced injuries in rats: A randomized controlled trial. Food and Chemical Toxicology.
524 2013;59(0):90-5.
525 3. Wang Y, Ma Y, Zheng Y, Song J, Yang X, Bi C, et al. In vitro and in vivo anticancer activity of a
526 novel puerarin nanosuspension against colon cancer, with high efficacy and low toxicity. Int J Pharm.
527 2013;441(1-2):728-35.
528 4. Hu W, Zhang Q, Yang X, Wang Y, Sun L. Puerarin inhibits adhesion molecule expression in
529 tnf-alpha-stimulated human endothelial cells via modulation of the nuclear factor kappaB pathway.
530 Pharmacology. 2010;85(1):27-35.
531 5. Chen R, Xue J, Xie M. Puerarin prevents isoprenaline-induced myocardial fibrosis in mice by
532 reduction of myocardial TGF-beta1 expression. J Nutr Biochem. 2012;23(9):1080-5.
533 6. Zhang S, Chen S, Shen Y, Yang D, Liu X, Sun-Chi AC, et al. Puerarin induces angiogenesis in
534 myocardium of rat with myocardial infarction. Biological & pharmaceutical bulletin. 2006;29(5):945-50.
535 7. Yan LP, Chan SW, Chan AS, Chen SL, Ma XJ, Xu HX. Puerarin decreases serum total cholesterol
536 and enhances thoracic aorta endothelial nitric oxide synthase expression in diet-induced
537 hypercholesterolemic rats. Life sciences. 2006;79(4):324-30.
538 8. Gao L, Ji X, Song J, Liu P, Yan F, Gong W, et al. Puerarin protects against ischemic brain injury in a
539 rat model of transient focal ischemia. Neurol Res. 2009;31(4):402-6.
540 9. Jin G, Yang P, Gong Y, Fan X, Tang J, Lin J. Effects of puerarin on expression of apelin and its
541 receptor of 2K1C renal hypertension rats. Zhongguo Zhong yao za zhi = Zhongguo zhongyao zazhi =
542 China journal of Chinese materia medica. 2009;34(24):3263-7.
543 10. Li H, Dong L, Liu Y, Wang G, Wang G, Qiao Y. Biopharmaceutics classification of puerarin and
544 comparison of perfusion approaches in rats. Int J Pharmaceut. 2014;466(1–2):133-8.
545 11. Tu L, Yi Y, Wu W, Hu F, Hu K, Feng J. Effects of particle size on the pharmacokinetics of puerarin
546 nanocrystals and microcrystals after oral administration to rat. Int J Pharm. 2013;458(1):135-40.
547 12. Tao HQ, Meng Q, Li MH, Yu H, Liu MF, Du D, et al. HP-beta-CD-PLGA nanoparticles improve the
548 penetration and bioavailability of puerarin and enhance the therapeutic effects on brain
549 ischemia-reperfusion injury in rats. Naunyn-Schmiedeberg's archives of pharmacology.
550 2013;386(1):61-70.
551 13. Zhao L, Liu A, Sun M, Gu J, Wang H, Wang S, et al. Enhancement of Oral Bioavailability of
552 Puerarin by Polybutylcyanoacrylate Nanoparticles. Journal of Nanomaterials. 2011;2011:1-8.
553 14. Luo CF, Yuan M, Chen MS, Liu SM, Zhu L, Huang BY, et al. Pharmacokinetics, tissue distribution
554 and relative bioavailability of puerarin solid lipid nanoparticles following oral administration. Int J Pharm.
555 2011;410(1-2):138-44.
556 15. Tang TT, Hu XB, Liao DH, Liu XY, Xiang DX. Mechanisms of microemulsion enhancing the oral
557 bioavailability of puerarin: comparison between oil-in-water and water-in-oil microemulsions using the
558 single-pass intestinal perfusion method and a chylomicron flow blocking approach. Int J Nanomedicine.
559 2013;8:4415-26.
560 16. Li Y, Pan WS, Chen SL, Xu HX, Yang DJ, Chan ASC. Pharmacokinetic, Tissue Distribution, and
561 Excretion of Puerarin and Puerarin-Phospholipid Complex in Rats. Drug Development and Industrial

562 Pharmacy. 2006;32(4):413-22.
563 17. Gao L, Liu G, Ma J, Wang X, Zhou L, Li X. Drug nanocrystals: In vivo performances. J Control
564 Release. 2012;160(3):418-30.
565 18. Keck CM, Muller RH. Drug nanocrystals of poorly soluble drugs produced by high pressure
566 homogenisation. European journal of pharmaceutics and biopharmaceutics : official journal of
567 Arbeitsgemeinschaft fur Pharmazeutische Verfahrenstechnik eV. 2006;62(1):3-16.
568 19. Mueller RH, Keck CM. Second generation of drug nanocrystals for delivery of poorly soluble drugs:
569 smartCrystal technology. Eur J Pharm Sci. 2008;34(1):S20-S1.
570 20. Wang Y, Ma Y, Ma Y, Du Y, Liu Z, Zhang D, et al. Formulation and pharmacokinetics evaluation of
571 puerarin nanocrystals for intravenous delivery. Journal of nanoscience and nanotechnology.
572 2012;12(8):6176-84.
573 21. Hu J, Ng WK, Dong Y, Shen S, Tan RB. Continuous and scalable process for water-redispersible
574 nanoformulation of poorly aqueous soluble APIs by antisolvent precipitation and spray-drying. Int J
575 Pharm. 2011;404(1-2):198-204.
576 22. Wasan EK, Bartlett K, Gershkovich P, Sivak O, Banno B, Wong Z, et al. Development and
577 characterization of oral lipid-based amphotericin B formulations with enhanced drug solubility, stability
578 and antifungal activity in rats infected with Aspergillus fumigatus or Candida albicans. Int J Pharm.
579 2009;372(1-2):76-84.
580 23. Li Y, Wang L, Tu Y, Yan J, Xu K, Li H. A new dosage form of emodin: For solubility and dissolution
581 rate enhancement and application in Alzheimer's disease and bacteriostasis. Journal of Drug Delivery
582 Science and Technology. 2015;29:261-8.
583 24. Zu Y, Sun W, Zhao X, Wang W, Li Y, Ge Y, et al. Preparation and characterization of amorphous
584 amphotericin B nanoparticles for oral administration through liquid antisolvent precipitation. Eur J Pharm
585 Sci. 2014;53:109-17.
586 25. Yan F, Zhang C, Zheng Y, Mei L, Tang L, Song C, et al. The effect of poloxamer 188 on
587 nanoparticle morphology, size, cancer cell uptake, and cytotoxicity. Nanomedicine: Nanotechnology,
588 Biology and Medicine. 2010;6(1):170-8.
589 26. Newa M, Bhandari KH, Li DX, Kwon T-H, Kim JA, Yoo BK, et al. Preparation, characterization and
590 in vivo evaluation of ibuprofen binary solid dispersions with poloxamer 188. Int J Pharmaceut.
591 2007;343(1–2):228-37.
592 27. Zu Y, Meng L, Zhao X, Ge Y, Yu X, Zhang Y, et al. Preparation of 10-hydroxycamptothecin-loaded
593 glycyrrhizic acid-conjugated bovine serum albumin nanoparticles for hepatocellular carcinoma-targeted
594 drug delivery. Int J Nanomedicine. 2013;8:1207-22.
595 28. J H, M D, D F, H V, K A. Preparation and characterization of nanocrystals for solubility and
596 dissolution rate enhancement of nifedipine. Int J Pharmaceut. 2005(1-2).
597 29. Affandi MM, Julianto T, Majeed A. Development and stability evaluation of Astaxanthin
598 Nanoemulsion. Asian Journal of Pharmaceutical and clinical research. 2011;4:142-48.
599 30. He W, Lu Y, Qi J, Chen L, Hu F, Wu W. Food proteins as novel nanosuspension stabilizers for
600 poorly water-soluble drugs. Int J Pharmaceut. 2013;441(1–2):269-78.
601 31. Li Y, Yang DJ, Zhou W, Chen SB, Chen SL. Recrystallization of puerarin using the supercritical
602 fluid antisolvent process. J Cryst Growth. 2012;340(1):142-8.
603 32. Kim JS, Kim MS, Park HJ, Jin SJ, Lee S, Hwang SJ. Physicochemical properties and oral
604 bioavailability of amorphous atorvastatin hemi-calcium using spray-drying and SAS process. Int J Pharm.
605 2008;359(1-2):211-9.

606 33. Dong Y, Ng WK, Hu J, Shen S, Tan RB. A continuous and highly effective static mixing process for
607 antisolvent precipitation of nanoparticles of poorly water-soluble drugs. Int J Pharm.
608 2010;386(1-2):256-61.
609 34. Mosharraf M, Nystrom C. Apparent solubility of drugs in partially crystalline systems. Drug Dev
610 Ind Pharm. 2003;29(6):603-22.
611 35. Kocbek P, Baumgartner S, Kristl J. Preparation and evaluation of nanosuspensions for enhancing the
612 dissolution of poorly soluble drugs. Int J Pharmaceut. 2006;312(1-2):179-86.
613 36. Kim S, Ng WK, Dong Y, Das S, Tan RB. Preparation and physicochemical characterization of< i>
614 trans</i>-resveratrol nanoparticles by temperature-controlled antisolvent precipitation. Journal of food
615 engineering. 2012;108(1):37-42.
616 37. Brough C, Williams RO, 3rd. Amorphous solid dispersions and nano-crystal technologies for poorly
617 water-soluble drug delivery. Int J Pharm. 2013;453(1):157-66.
618

619

620 **Figure legends**

621 Fig.1. The flow chart of the experimental processes.

622 Fig.2. Effect of six main factors on the MPS of PUE emulsions. (a) the volume ratio of water to
623 organic phase; (b) the concentration of poloxamer 188; (c) homogenized speed; (d) homogenized
624 time; (e) high-pressure homogenization pressure; (f) high-pressure homogenization cycles.

625 Fig.3. SEM pictures of (a) raw PUE powder and (b) PUENs powder; the normal distribution curves
626 of PUENs (c_1) before and (d_1) after the freeze-drying; the light microscopy images of the
627 nanosuspensions (c_2) before and (d_2) after the freeze-drying (10×40).

628 Fig.4. TEM image of PUENs.

629 Fig.5. Infrared spectrograms of (a) raw PUE; (b) PUENs; (c) MIX-PUE; (d) poloxamer 188.

630 Fig.6. A: XRD patterns of (a) PUENs; (b) raw PUE; (c) MIX-PUE; (d) poloxamer 188. B:
631 Crystalline states of PUENS at (e) 0 d; (f) 180 d; (g) 365 d.

632 Fig.7. DSC thermograms of (a) PUENs; (b) raw PUE; (c) MIX-PUE; (d) poloxamer 188.

633 Fig.8. TGA thermograms of (a) PUENs; (b) raw PUE; (c) MIX-PUE; (d) poloxamer 188.

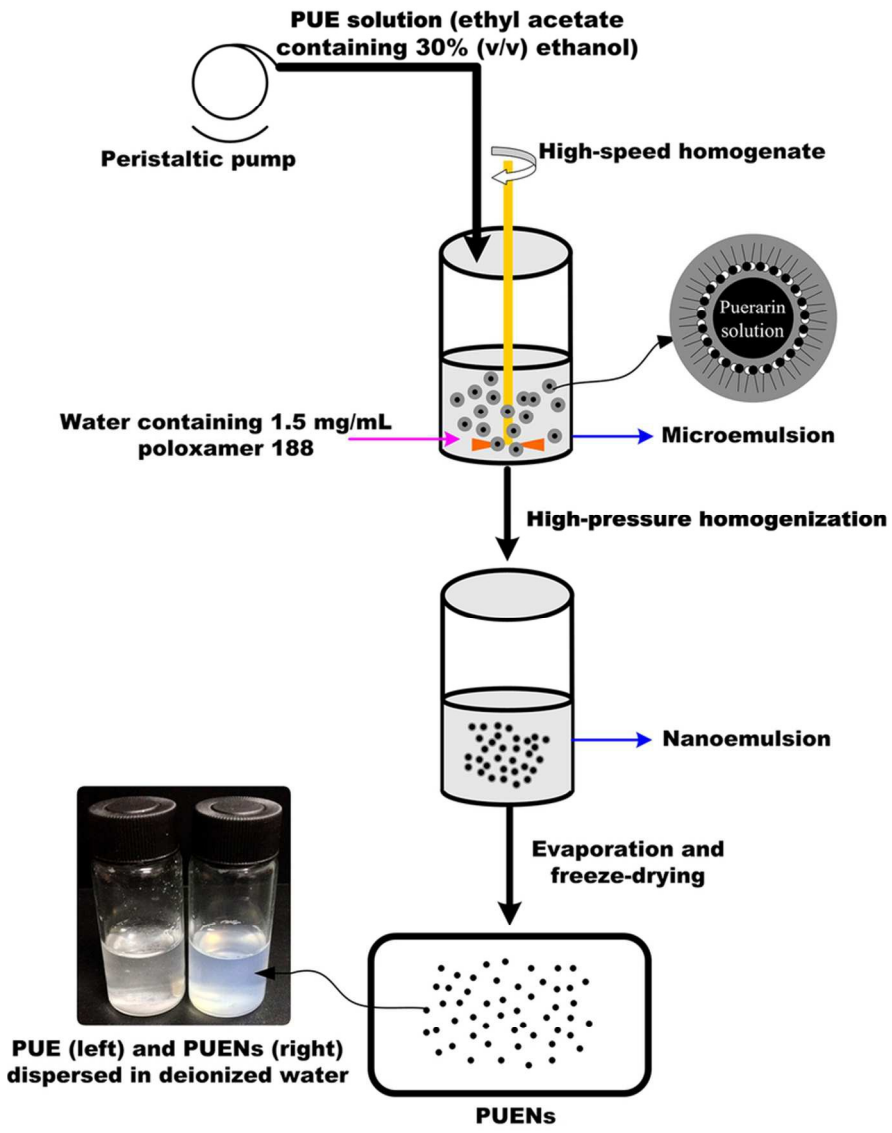

Fig.1. The flow chart of the experimental processes.
Fig. 1
82x93mm (300 x 300 DPI)

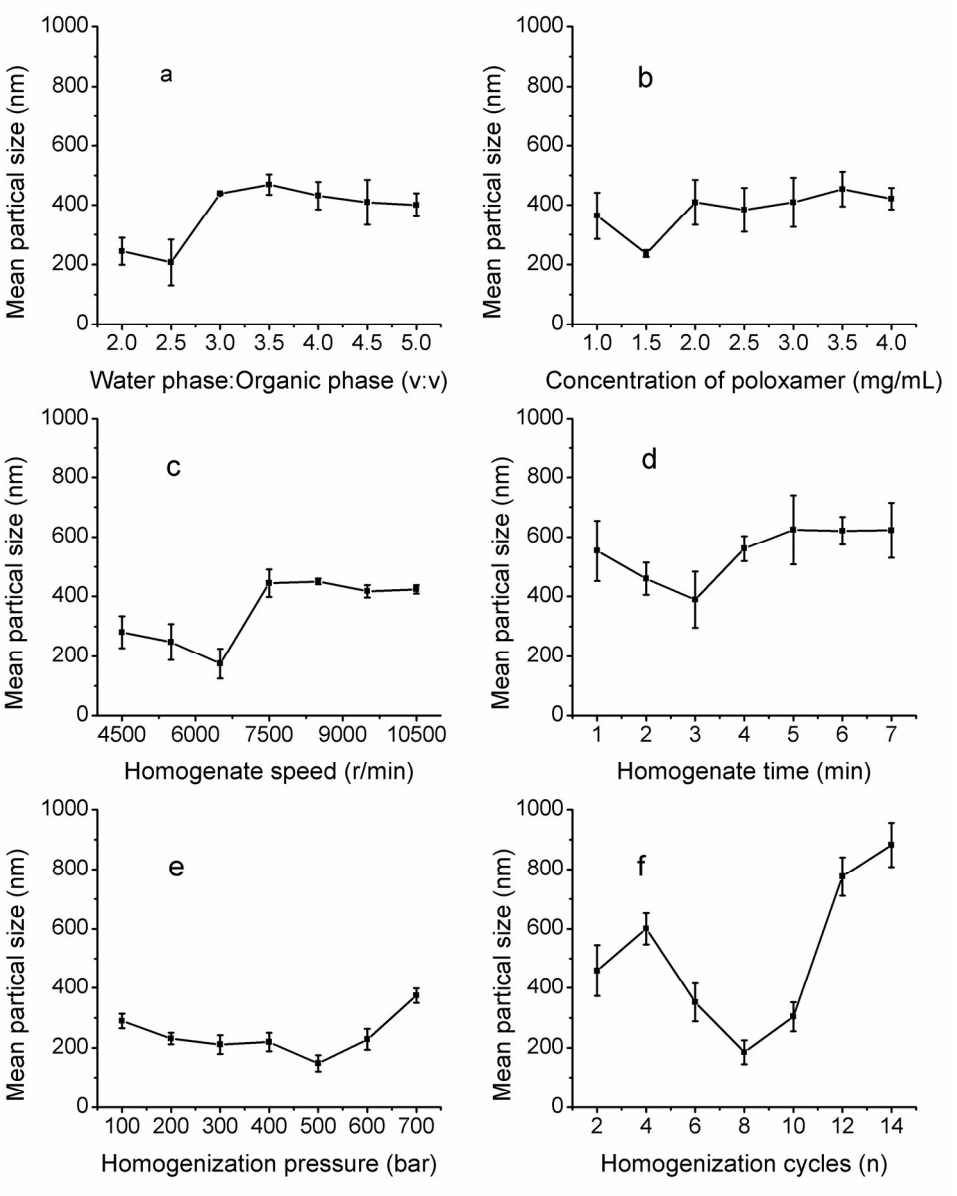

Fig.2. Effect of six main factors on the MPS of PUE emulsions. (a) the volume ratio of water to organic phase; (b) the concentration of poloxamer 188; (c) homogenized speed; (d) homogenized time; (e) high-pressure homogenization pressure; (f) high-pressure homogenization cycles.

Fig. 2

84x106mm (600 x 600 DPI)

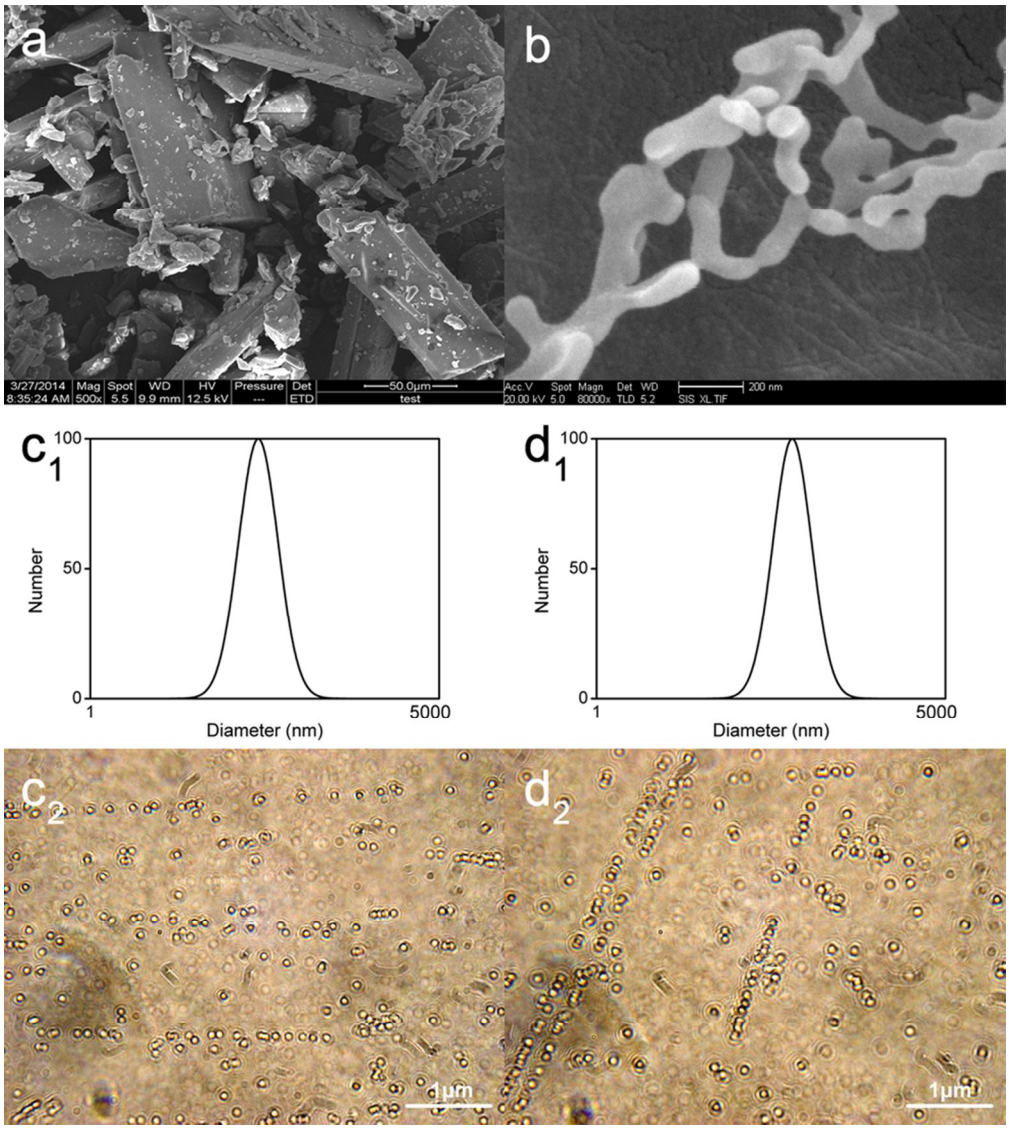

Fig.3. SEM pictures of (a) raw PUE powder and (b) PUENs powder; the normal distribution curves of PUENs (c1) before and (d1) after the freeze-drying; the light microscopy images of the nanosuspensions (c2) before and (d2) after the freeze-drying (10×40).

Fig. 3

82x92mm (300 x 300 DPI)

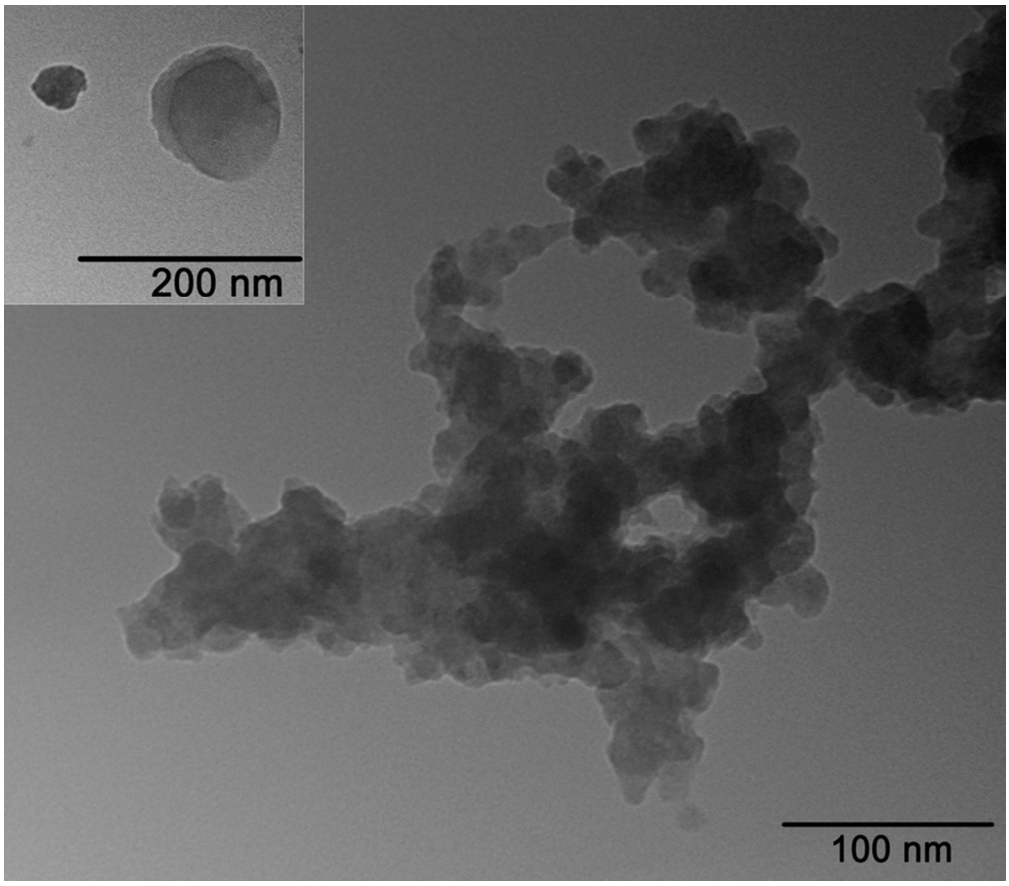

Fig.4. TEM image of PUENs.
Fig. 4
73x64mm (300 x 300 DPI)

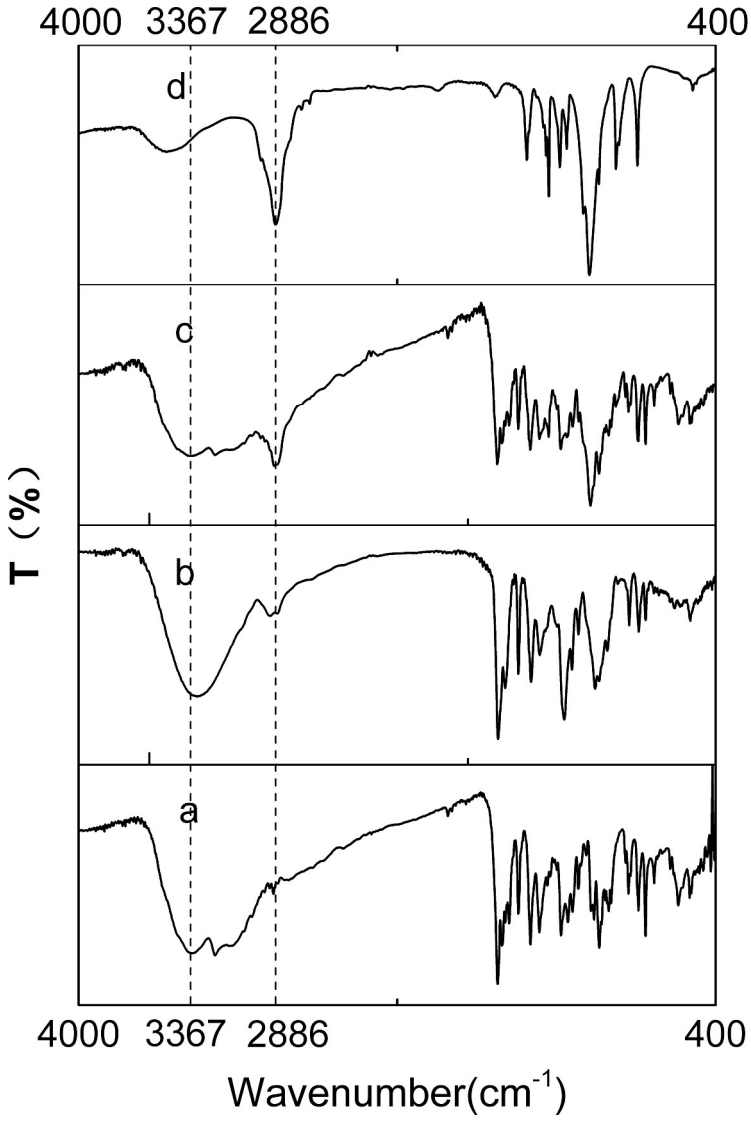

Fig.5. Infrared spectrograms of (a) raw PUE; (b) PUENs; (c) MIX-PUE; (d) poloxamer 188.
Fig. 5
134x190mm (600 x 600 DPI)

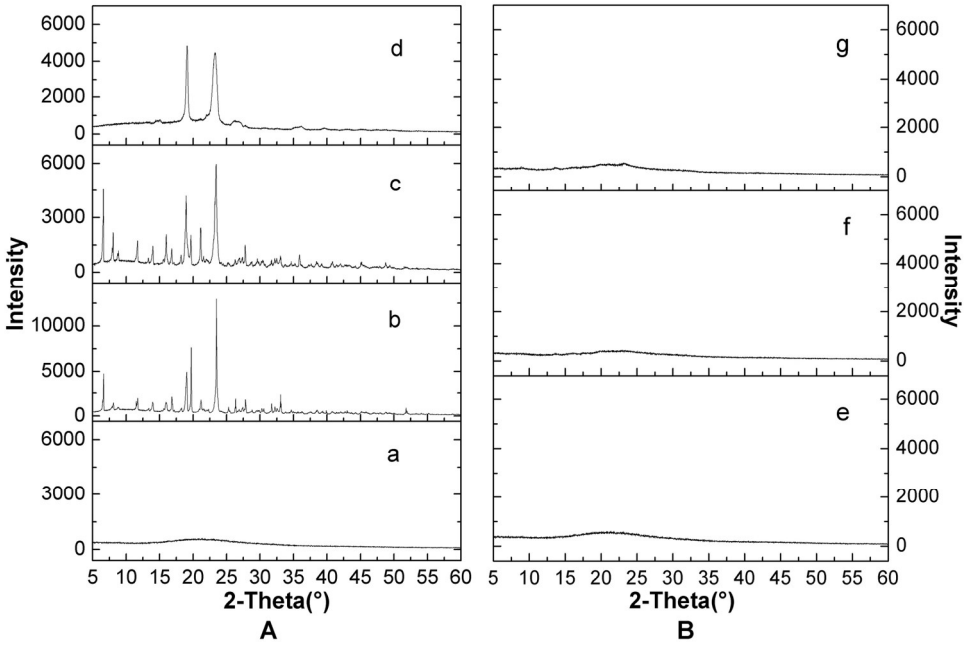

Fig.6. A: XRD patterns of (a) PUENs; (b) raw PUE; (c) MIX-PUE; (d) poloxamer 188. B: Crystalline states of PUENS at (e) 0 d; (f) 180 d; (g) 365 d.
Fig. 6
76x61mm (600 x 600 DPI)

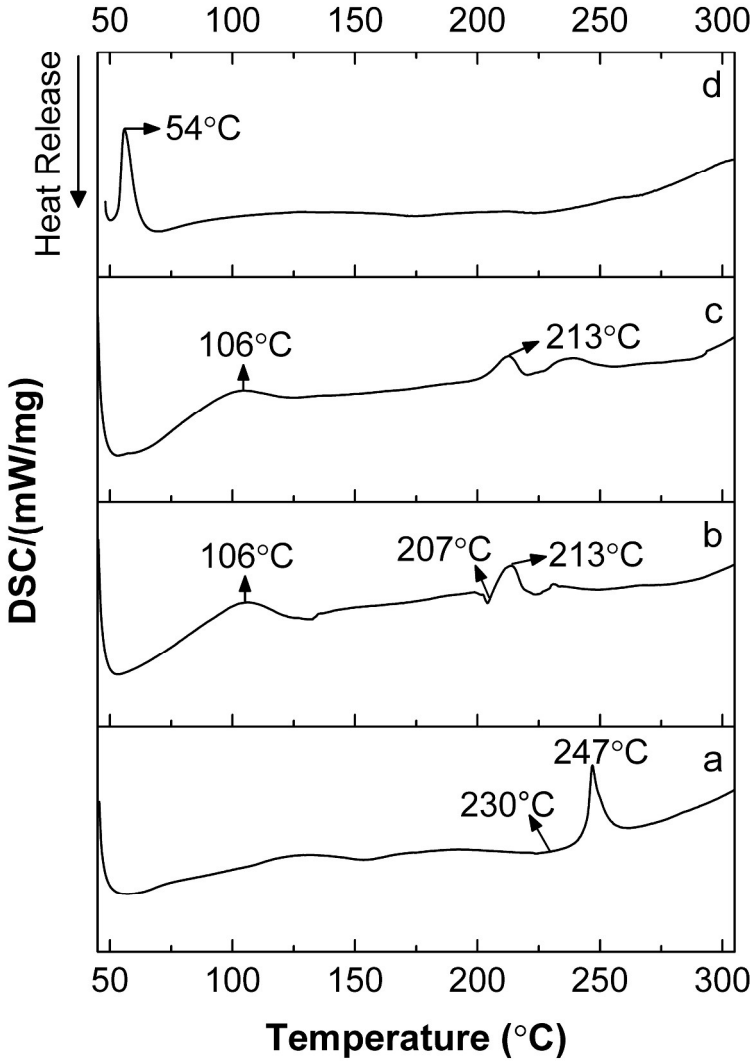

Fig.7. DSC thermograms of (a) PUENs; (b) raw PUE; (c) MIX-PUE; (d) poloxamer 188.
Fig. 7
134x190mm (600 x 600 DPI)

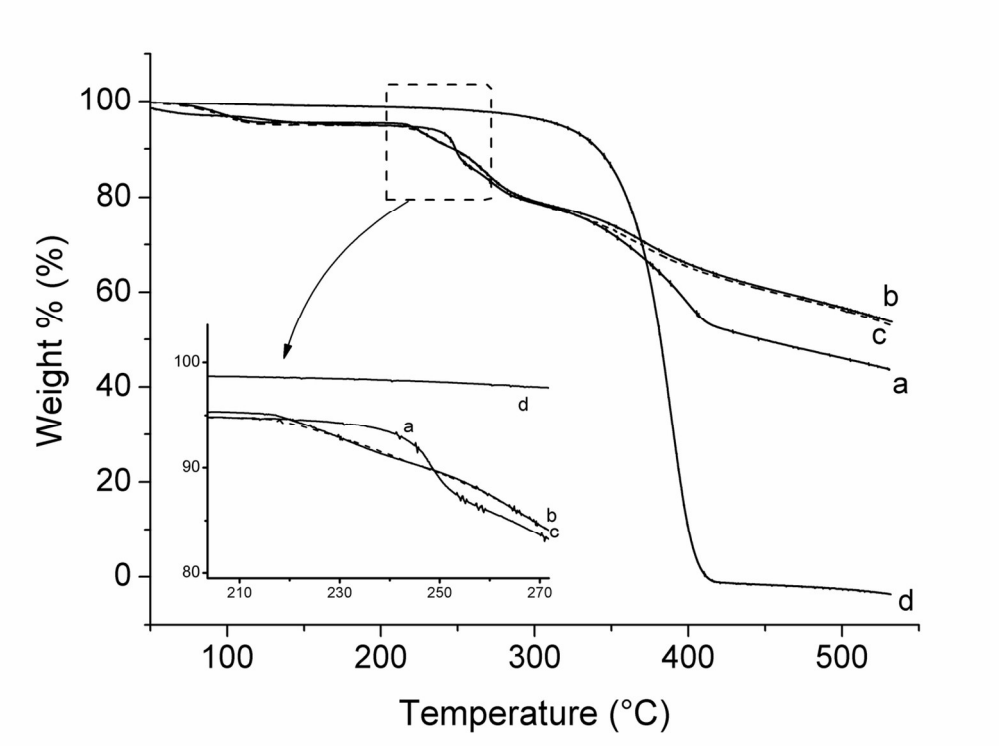

Fig.8. TGA thermograms of (a) PUENs; (b) raw PUE; (c) MIX-PUE; (d) poloxamer 188.
Fig. 8
63x47mm (600 x 600 DPI)

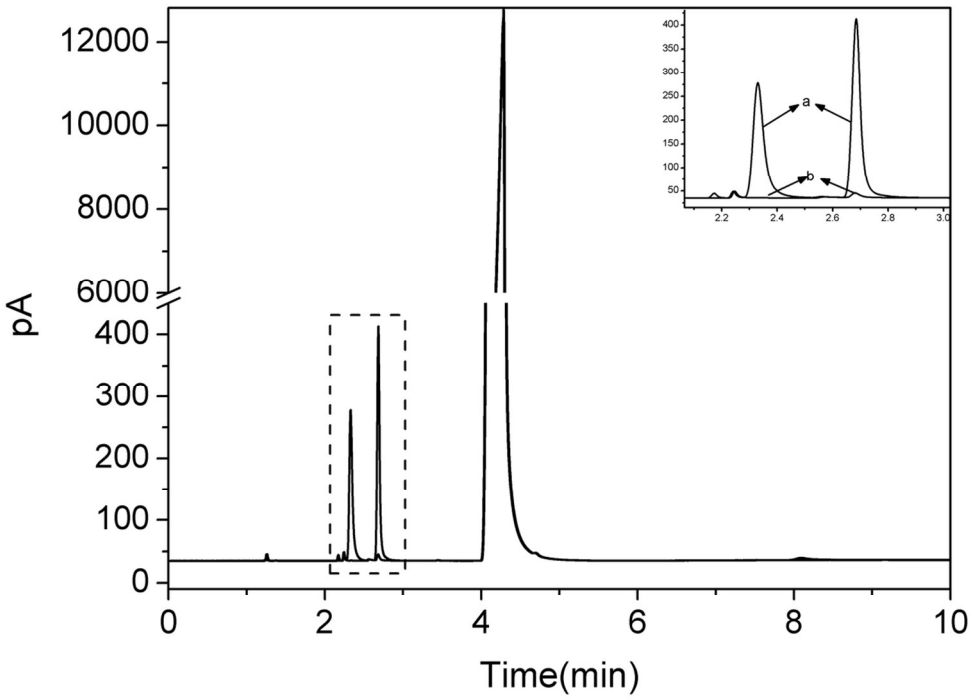

Fig.9. Gas chromatograms of (a) ethyl acetate and ethanol standard solution; (b) PUENs solution.
Fig. 9
56x41mm (600 x 600 DPI)

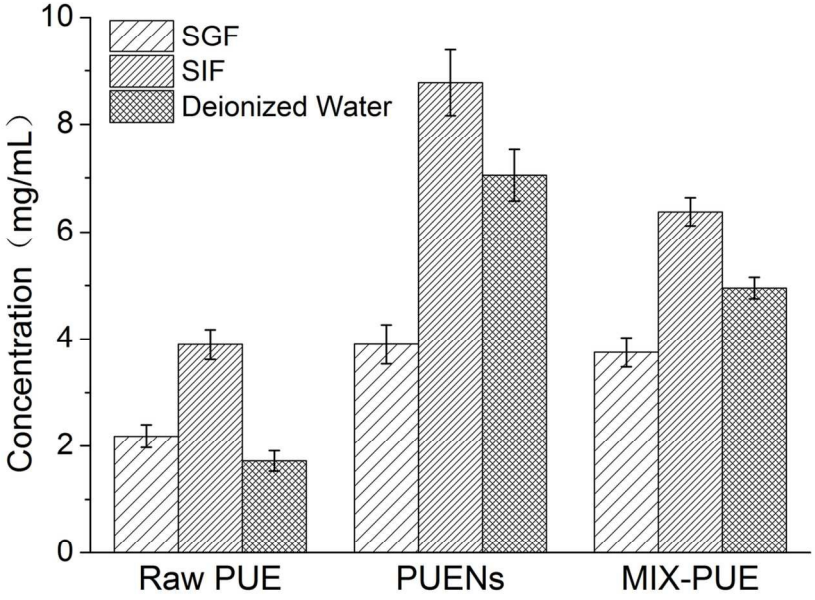

Fig.10. Equilibrium solubility in SGF, SIF and deionized water.
Fig. 10
58x41mm (600 x 600 DPI)

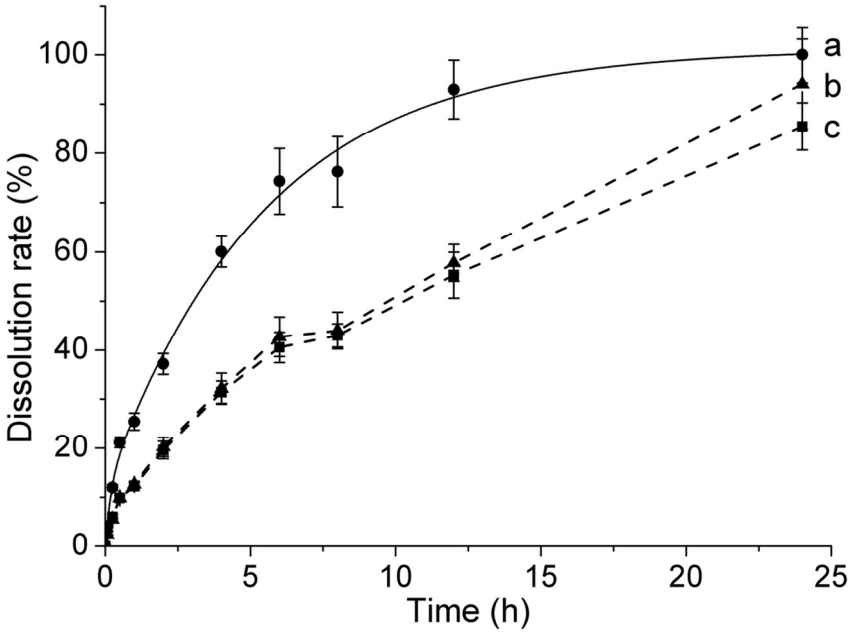

Fig.11. Dissolution rate in SGF (a) PUENs; (b) MIX-PUE; (c) raw PUE.
Fig. 11
58x41mm (600 x 600 DPI)

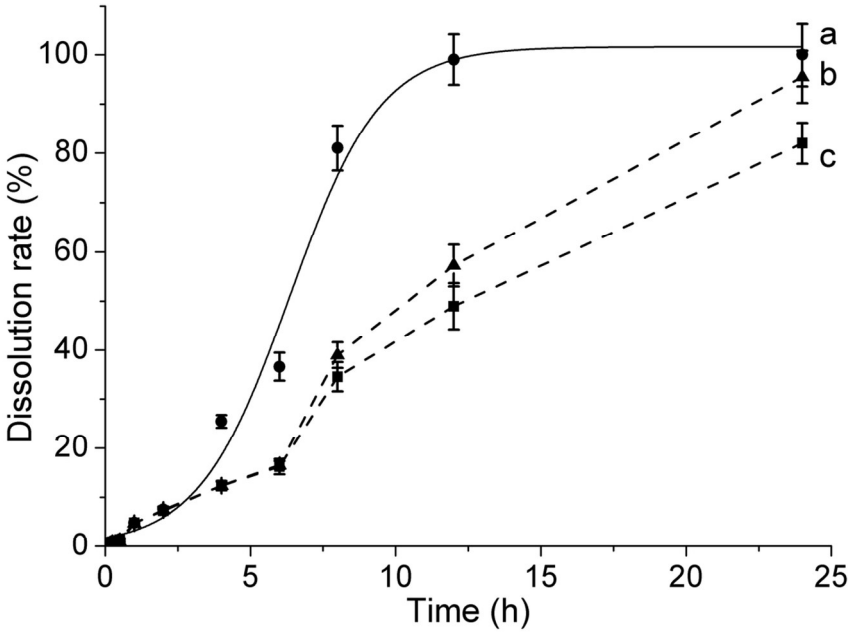

Fig.12. Dissolution rate in SIF (a) PUENs; (b) MIX-PUE; (c) raw PUE.
Fig. 12
58x41mm (600 x 600 DPI)

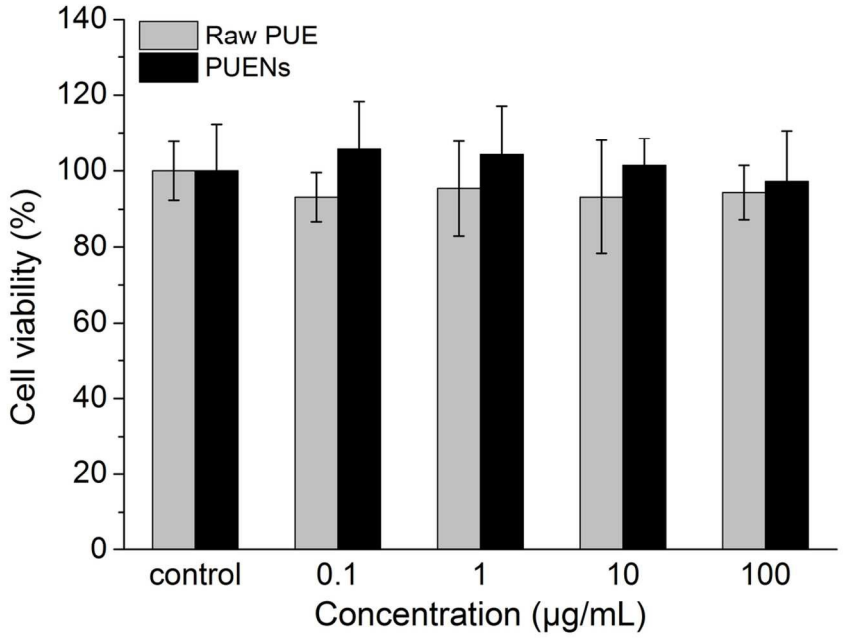

Fig.13. Effect of raw PUE and PUENs on IEC-6 cell viability
Fig. 13
58x41mm (600 x 600 DPI)

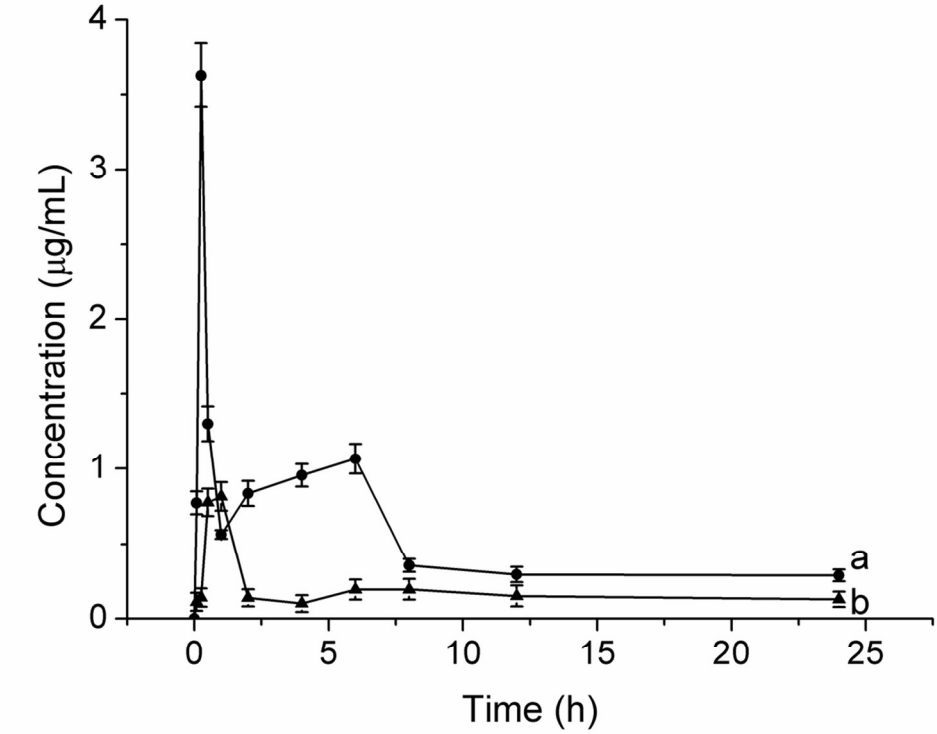

Fig.14. Concentration-time curves of (a) PUENs; (b) raw PUE.
Fig. 14
54x40mm (600 x 600 DPI)

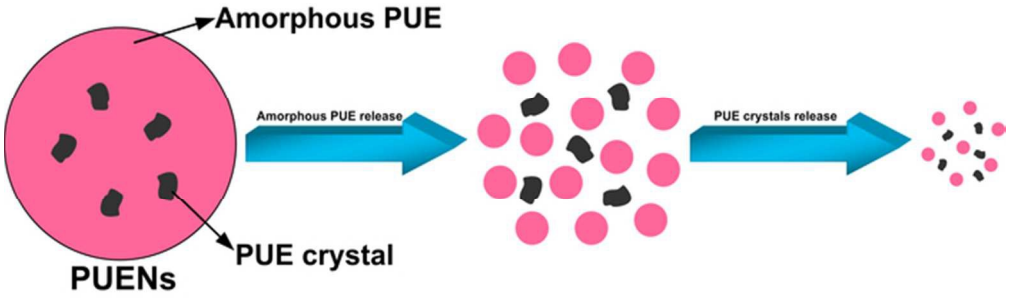

Fig.15. Schematic diagram of in vivo drug release mechanism
Fig. 15
59x17mm (300 x 300 DPI)

Table 1: Relationships between parameters and mean particle size in single-factor method

Variable	level	Mean particle size(nm)±SD	CV
Ratios of water to oil phase (v/v)	2:1	244.9 ± 45.8	
	2.5:1	207.5 ± 76.8	
	3:1	438.9 ± 2.3	
	3.5:1	469.0 ± 34.4	27.5%
	4:1	431.8 ± 46.1	
	4.5:1	409.8 ± 75.7	
	5:1	400.4 ± 38.7	
Concentration of poloxamer 188 (mg/mL)	1	363.6 ± 77.6	
	1.5	236.9 ± 11.9	
	2	409.1 ± 75.7	
	2.5	384.2 ± 73.6	18.4%
	3	409.5 ± 82.6	
	3.5	453.9 ± 58.9	
	4	421.4 ± 35.8	
Homogenate speeds (rpm)	4500	280.4 ± 53.9	
	5500	247.7 ± 60.4	
	6500	174.7 ± 49.9	
	7500	444.4 ± 45.8	32.1%
	8500	450.1 ± 9.7	
	9500	417.4 ± 20.9	
	10500	423.7 ± 14.5	
Homogenate time (min)	1	552.9 ± 100.9	
	2	459.6 ± 54.1	
	3	389.3 ± 94.3	
	4	560.6 ± 42.0	42.6%
	5	624.1 ± 116	
	6	620.5 ± 46.2	
	7	622.4 ± 92.1	
Homogenization pressure (bar)	100	289.5 ± 24.0	
	200	231.1 ± 19.1	
	300	210.9 ± 31.5	
	400	219.0 ± 30.8	29.2%
	500	148.4 ± 27.1	
	600	228.1 ± 34.6	
	700	374.3 ± 23.9	
Homogenization times	2	458.7 ± 85.9	
	4	600.2 ± 53.1	
	6	352.2 ± 63.5	
	8	185.2 ± 39.8	50.4%
	10	304.1 ± 48.5	
	12	776.6 ± 64.5	
	14	882.5 ± 73.6	

Table 2: *In vivo* parameters of the raw PUE and PUENs

Parameter	Unit	Raw PUE	PUENs
C_{max}	mg/L	0.81	3.63
T_{max}	h	1	0.25
$AUC_{(0-t)}$	mg/L·h	4.31	12.20
$AUC_{(0-\infty)}$	mg/L·h	9.75	16.69
K_{10}	1/h	0.35	1.00
K_{12}	1/h	1.92	7.92
K_{21}	1/h	0.10	0.50

Table 3: Effects of raw PUE and PUENs on hemorheology in rats (n=10, $\bar{x} \pm SD$)

Measured parameter		Control	Raw PUE	PUENs
Whole blood viscosity (mPa·s)	$10s^{-1}$	8.38 ± 0.28	8.02 ± 0.76	6.56 ± 1.12*
	$60s^{-1}$	4.98 ± 0.13	4.55 ± 0.19	4.09 ± 0.53*
	$150s^{-1}$	3.97 ± 0.14	3.72 ± 0.17	3.36 ± 0.36*
Plasma viscosity (mPa·s)	$120s^{-1}$	1.18 ± 0.16	1.30 ± 0.22	1.20 ± 0.22
Hematocrit (%)		36.00 ± 3.46	36.13 ± 1.81	35.00 ± 1.94
Whole blood reduced viscosity	$10s^{-1}$	20.10 ± 1.99	18.69 ± 2.68	15.26 ± 2.47*
(mPa·s)	$60s^{-1}$	10.61 ± 0.98	9.03 ± 1.16	8.26 ± 1.34*
	$150s^{-1}$	7.79 ± 0.69	6.75 ± 1.00	6.17 ± 0.94*
Erythrocyte aggregation index		2.11 ± 0.12	2.16 ± 0.16	1.94 ± 0.14
Erythrocyte rigidity index		6.61 ± 0.37	5.41 ± 1.48	5.34 ± 1.37
Erythrocyte deformation index		1.07 ± 0.04	0.96 ± 0.15	0.97 ± 0.15
Erythrocyte electrophoresis index		5.90 ± 0.58	5.98 ± 0.64	5.55 ± 0.32

*$p<0.05$ vs. control group

Preparation, characterization and bioavailability of oral puerarin nanoparticles by emulsion solvent evaporation method

Yin Zhang, Yong Li, Xiuhua Zhao*, Yuangang Zu[1*], Weiguo Wang, Weiwei Wu, Chen Zhong, Zhao Li

(Key Laboratory of Forest Plant Ecology, Northeast Forestry University, Ministry of Education, Harbin 150040, Heilongjiang, China)

Graphical Abstract:

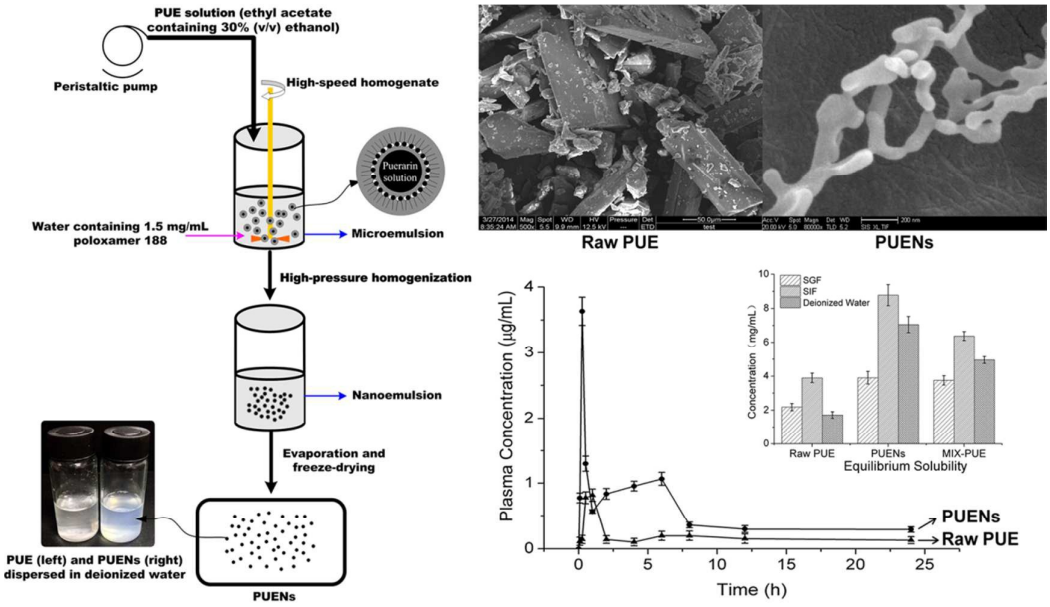

To improve the water solubility and dissolution rate, puerarin (PUE) was nanocrystallized by an emulsion solvent evaporation (ESE) method, followed by freeze-drying. The solubility, dissolution rate and oral bioavailability of PUENs were significantly improved compared with raw PUE. According to the results above, PUENs show the potential application value on its oral absorption.

* Corresponding author. Tel.: +86-451-82191517; fax: +86-451-82102082.
E-mail address: xiuhuazhao@nefu.edu.cn (Xiuhua Zhao).
* Corresponding author. Tel.: +86-451-82191517; fax: +86-451-82102082.
E-mail address: yuangangzu@163.com (Yuangang Zu)